



LIGHT CURVE CHARACTERISTICS OF GAMMA-RAY BURSTS

By

Temam Beyan

**A THESIS SUBMITTED TO
GRADUATE PROGRAMS OF
ADDIS ABABA UNIVERSITY
IN PARTIAL FULFILLMENT FOR THE REQUIREMENTS
OF THE DEGREE
MASTER OF SCIENCE IN PHYSICS
(ASTRONOMY/ASTROPHYSICS)
ADDIS ABABA, ETHIOPIA
SEPTEMBER 2022**

ADDIS ABABA UNIVERSITY
PROGRAM OF GRADUATE STUDIES

LIGHT CURVE CHARACTERISTICS OF GAMMA-RAY BURSTS

By
Temam Beyan
Department of Physics
Addis Ababa University

Approved by the Examining Board:

Dr. Firaol Fana
Advisor

Signature

Examiner

Signature

Examiner

Signature

Date: September 2022

ADDIS ABABA UNIVERSITY

Date: **September 2022**

Author: **Temam Beyan**

Title: **Light Curve Charactersics Of Gamma-Ray Bursts**

Department: **Department of Physics**

Degree: **M.Sc.** Convocation: **April** Year: **2021**

Permission is herewith granted to Addis Ababa University to circulate and to have copied for non-commercial purposes, at its discretion, the above title upon the request of individuals or institutions.

Signature of Author

THE AUTHOR RESERVES OTHER PUBLICATION RIGHTS, AND NEITHER THE THESIS NOR EXTENSIVE EXTRACTS FROM IT MAY BE PRINTED OR OTHERWISE REPRODUCED WITHOUT THE AUTHOR'S WRITTEN PERMISSION.

THE AUTHOR ATTESTS THAT PERMISSION HAS BEEN OBTAINED FOR THE USE OF ANY COPYRIGHTED MATERIAL APPEARING IN THIS THESIS (OTHER THAN BRIEF EXCERPTS REQUIRING ONLY PROPER ACKNOWLEDGEMENT IN SCHOLARLY WRITING) AND THAT ALL SUCH USE IS CLEARLY ACKNOWLEDGED.

This Work is Dedicated

to

*My brothers Mulugeta Asfie and Kalamlak Azanaw died
in 1995 / 1997 E.C*

Table of Contents

Table of Contents	v
List of Table	vii
List of Figures	viii
Acknowledgements	x
Abbreviations	xi
Physical Constants	xii
Symbols	xiii
Abstract	xiv
1 Physics of gamma-ray bursts.	1
1.1 Introduction	1
1.2 Historical Discovery of gamma-Ray bursts	2
1.2.1 Dark era (1967-1990)	2
1.2.2 BATSE era (1991-2000)	4
1.2.3 BeppoSAX era (1997-2000)	5
1.2.4 Swift era (2004-now)	6
1.2.5 Fermi era (2008-now)	8
1.3 Classification of gamma-ray bursts	8
1.3.1 short/hard gamma-ray bursts	9
1.3.2 long/soft gamma-ray bursts	10
1.3.3 Ultra long gamma-ray bursts (ULGRBs)	10
1.4 Global properties of GRBs	10
1.4.1 Intensity distribution	10
1.4.2 Angular distribution	11
1.5 Statement of the problems	12

1.6	Objectives and thesis outline	12
2	Emission mechanisms and observational properties of gamma-ray bursts	14
2.1	GRBs production mechanisms	14
2.1.1	Basic fireball model	14
2.1.2	GRBs progenitors models	21
2.1.3	Working mechanisms of central engine	21
2.1.4	GRB-SN assocition	22
2.2	GRBs Obsevation and interpretations	22
2.2.1	prompt GRB emission	23
2.2.2	Afterglow GRB emission	24
2.3	Interpretations of GRBs afterglow	25
2.3.1	Late time afterglows	26
2.4	Theoritical interpretation of X-ray afterglow	27
2.4.1	Steep decay of early x-ray light curves	27
2.4.2	Shallow /plateau decay X-ray light curves	28
2.4.3	normal decay of x-ray light curve	29
2.4.4	Late steep decay following the plateau in X-ray light curves .	29
2.4.5	Time breaks in swift X-ray afterglow	30
2.4.6	The first break in the light curve ($t_{break,1}$)	30
2.5	Decay of flux with time of observed light currve	30
3	Research methodology	33
3.1	Research designs	33
3.2	Type of data and its source	35
3.3	Data sampling technique and size	35
3.4	Validity and reliability of data	35
3.5	Data processing and analyzing	36
3.5.1	Data processing	36
3.5.2	Data analyzing	36
4	Result and discussion	37
4.1	Results	37
4.2	discussion	37
5	Conclusion	38

Bibliography	39
Bibliography	40

List of Tables

3.1	classes of sampled GRBs with light curve(s): 1,2 and 3 breaks	35
-----	---	----

List of Figures

1.1	Light curve of the first GRB ever detected by Vela. Two separate pulses can be identified over a duration of less than 10 seconds [?] .	3
1.2	The distribution of all 2704 GRBs detected by BATSE satellite: they are clearly isotropic distribution . [?]	5
1.3	Schematic view of the swift satellite(Gehrels et.al 2004).The size of Mask of BAT is $2.7m^2$ [?]	7
1.4	The GRB classification (long and short) distribution. GRBs last between a few milliseconds and several minutes. There appear to be two populations, 'short' bursts, with duration peaking around 0.3 seconds and 'long' bursts, which last around 30 seconds, with the 'dividing line' between the groups being 2 seconds.	9
2.1	Visualization of the fireball model that illustrates the various steps of basic standard model with the internal and external shocks and radiations. At the left the two main scenarios (collapser and merger) indicated that they lead to a central black hole surrounded by a disk. (from Gehrels et al. (2002), credit Juan Velasco)[?]	16
2.2	Standard fireball model.	18
2.3	Qualitative schematic view of the structure of the relativistic jet produced by the gamma-ray burst. The external shock arises as a result of the impact of the jet on the stellar wind of the progenitor. This is where the final goodbye of the SOS similar emission from the collapsing star forms, which is characterized by a smooth (but non-monotonic) light variation. The internal shock persists as long as the central engine continues operating this is where rapidly varying gamma-, x-ray, and optical radiation forms.	19

2.4	Schematic scenarios for plausible progenitors of long and short GRB. The exact nature of the GRB progenitors is unknown, although it is possible that long GRBs come from the collapse of massive, rapidly rotating stars and short GRBs result from the merger of compact objects.	22
2.5	(a) Collapser model that show internal and external shocks producing prompt and afterglow emissions respectively. (b) Schematic evolution of the jet Lorentz factor and examples of symbolic locations of radius: the saturation radius r_s , photo spheric radius r_{ph} , internal shock radius r_{is} and external shock r_{es}	24
2.6	Diverse light curves of the GRBs prompt emission detected by BATSE instrument. This sample includes short and long events. https://gammaray.nsstc.nasa.gov	
2.7	(a) Canonical GRB light curve , showing prompt phase followed by afterglow phase. (b) Canonical x-ray light curves with its components: a steep decay phase (typical index of 3) which can then break to a shallower decline (shallow decay phase), a standard afterglow phase (pre-jet break phase), and possibly, a jet break and post-jet break phase. Sometimes an X-ray flare is seen.	28
2.8	A sketch of the various angles and distances for the large angle (or high latitude) emission when the γ -ray source turns off suddenly. . .	31

Acknowledgements

First of all, I thanks to God for His unlimited love, care, and undesirable help He has done to me throughout my life. I would like to express my deep gratitude to my advisor and instructor Dr. Remudin Reshid for his continuous guidance and great support. I would like to extend my thanks to my instructors and the department of physics of the Addis Ababa University and its staffs, I have learned many things from them like respecting teaching profession, punctuality, encouraging learners to have creative mind and so on. I would also like to acknowledge the financial support for my studies provided by the Addis Ababa Educational Bureau. Finally, I am very grateful thanks to my friends Murad Yimam, Debela Alemayehu, Jemal Regassa, Natnael and all my classmates I have received many comments and feed backs.

Addis Ababa University

Temam Beyan

April, 2021

Abbreviations

ASD	Amplitude Spectral Density
AXPs	Anomalous X-Ray Pulsars
EFE	Einstein Field Equation
BBH	Binary Black hole
BBN	Big Bang Nucleosynthesis
BHNS	Black hole Neutron Star
CBC	Compact Binary Coalescence
CMBR	Cosmic Microwave Background Radiation
CW	Continuous Wave
PN	Post Newtonian
GRBs	Gama-ray Bursts
GR	General Relativity
GW	Gravitational Wave
LIGO	Laser Interferometer Gravitational Wave Observatory
LISA	Laser Interferometer Space Astronomy
MBH	Massive Black hole
NR	Numerical Relativity
SEOBNR	Spin Effective One Body Numerical Relativity
IMRPhenom	In-spiral Merge Ringdown Phenomenological
PSDs	Power Spectral Density
SGRS	Soft Gama-ray Repeaters
SNR	Signal to Noise Ratio

Physical Constants

Speed of Light	$C = 2.99792458 \times 10^8 \text{ ms}^{-2}$
Universal Gravitational Constant	$G = 6.67 \times 10^{-11} \text{ Nm}^2 \text{ kg}^{-2}$
Mega parsec	$\text{Mpc} = 3.08568025 \times 10^{24} \text{ cm}$
Planck luminosity	$L_0 = 10^{59} \text{ egr/s}$
Mass of the Sun	$M_{\odot} = 1.99 \times 10^{33} \text{ g}$
Kilo parsec	$\text{kpc} = 3.08568025 \times 10^{21} \text{ cm}$
luminosity of the Sun	$L_{\odot} = 3.839 \times 10^{33} \text{ erg/s}$
Positive Cosmological constant	$\Lambda = (10^{16} \text{ ly})^{-2}$
Hubble's constant	$H_0 = 70.65 \text{ km/s/Mpc}$

Symbols

f_{GW}	Gravitational Wave frequency in Hz
L	Total radiated luminosity in erg/s
τ	Time remaining before coalescence in second(s)
M_c	Chirp mass in M_\odot
ρ_{crit}	Critical energy density in eV/cm^3
D_l	Luminosity distance of the from the source to Earth in Mpc
S_{GW}	Power spectral density in unit of egr/sHz

Abstract

Physics of gamma-ray bursts.

1.1 Introduction

what are gamma-ray bursts?

Gamma-Ray Bursts (GRBs) are the most explosive events in the Universe since the Big Bang. They are characterized by Sudden ,intense , bright and non-repeative flashes of gamma-ray photons of energy in the gamma -ray band (keV - GeV) lasting from a few tens of milliseconds to several minutes.They are the fastest extended objects of Nature, that injecting large amount of energy of order 10^{54} ergs or 10^{47} joules from very small compact region in a few seconds at cosmological distance.The energy they released for a few second to hundred seconds comparable to the energy that the Sun will emit in its entire 10 billion years of life time. Furthermore,the overall observed fluence ranges from 10^{-4} ergs/ cm^2 to 10^{-7} ergs/ cm^2 (see fig 1.2 in section 1.2), and corresponds to the isotropic equivalent luminosity of 10^{48} to 10^{54} erg s^{-1} [?].

Gamma Ray Bursts (GRBs) are at the intersection of many different areas of astrophysics: they are relativistic events connected with the end stages of massive stars; they reveal properties of their surrounding medium and of their host galaxies; they emit radiation from gamma-rays to radio wavelengths, as well as possibly non-electromagnetic signals, such as neutrinos, cosmic rays and gravitational waves. Due to their enormous luminosity, they can be detected even if they occur at vast distances, and are therefore also of great interest for cosmology [?].

During explosions, ultra relativistic jets are produced accompanied by an intense gamma-ray flashes called prompt emissions that outshine all the sky at very high red shifts.These prompt emissions are often followed by afterglow signals across the electromagnetic spectrum from X-ray to radio wavelengths covering timescales from tenth of seconds up to several months or more [? ?].

GRB events are classified as being either long (lasting > 2) or short (lasting < 2 s), separated by the length of duration $T_{90} \sim 2\text{sec}$, and spectral hardness of their prompt emissions, with long GRBs (LGRBs) believed to be associated with the deaths of collapsed massive stars, whilst short GRBs (SGRBs) more likely to be the result of either the merger of binary neutron stars (BNS) or the merger of a neutron star with a black hole (NS-BH) [?].

Due to their huge radiated energies, GRBs can be observed up to $z \sim 10$, therefore they are very powerful cosmological tools, complementary to other probes such as SN-Ia , clusters etc. The correlation between spectral peak photon energy $E_{p,i}$ and intensity (E_{iso} , L_{iso} , $L_{p,iso}$) is one of the most robust and intriguing properties of GRBs and a promising tool for measuring cosmological parameters [? ?].

1.2 Historical Discovery of gamma-Ray bursts

Gamma-ray bursts (GRBs) were first discovered unexpectedly during the Cold War in the late of 1960s by the Vela military satellites that were equipped with detectors of gamma-rays, X-rays and neutrons and launched by USA Air Force in collaboration with the Los Alamos National Laboratory. The first event was recorded in 1967. After verification, it was clear that gamma radiation was not of human origin, nor even terrestrial. However, the existence of Gamma-ray flashes coming from cosmos was announced the first event after six years in 1973 dating back to July 2, 1967 [?].

The study of GRBs physics mainly led by observations with help of improved detecting instruments on satellites to monitor phenomena in the universe in relation to Gamma-ray emissions. Prompted by the instrumental progress from time to time, the story of observational research of GRBs from early time to recent classified in five eras [?] [?].

1.2.1 Dark era (1967-1990)

The first gamma-ray burst discovered named as " GRB 670702" that detected by Vela satellite (see fig 1.1). In the name " GRB 670702", the first two digits represent

the burst year, the middle two and the last two digits represent month and the last two digits date of the burst. If more than two events of bursts were happened in one day, they labeled to identify them using English letters alphabetically. [?] [?].

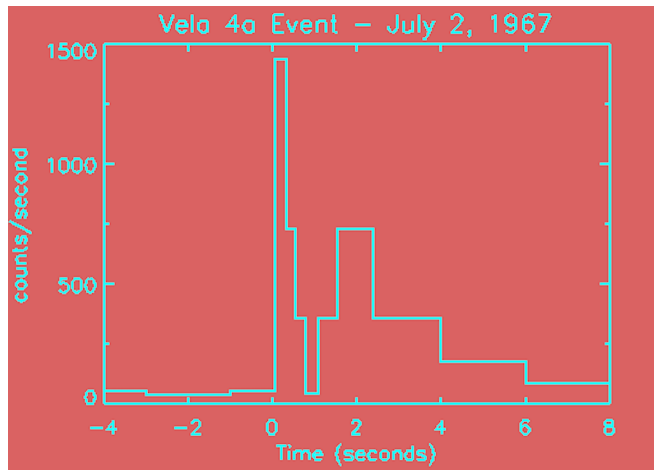


Figure 1.1: Light curve of the first GRB ever detected by Vela. Two separate pulses can be identified over a duration of less than 10 seconds [?]]

After the first discovery , the series of vela satellites were launched ,and more than 70 GRBs were detected. These earliest observational result of GRBs only consists several structures “spikes” were found in Gamma-ray band ,but no way to identify their location. However,after series of vela satellites were launched with improved detecting instruments ,the origins of GRBs believed to be out side the solar system by offset information [?]] [?].

The fundamental questions of the era were : Where are GRBs come from ? What is the source of such flashes of light? By what mechanisms ? do they appear in our galaxy, the Milky Way, or in more distant galaxies ? To answer such questions More than one hundred models were proposed to explain the origin and production mechanisms of GRBs. However, only a few of them were explaining that GRBs events occur at cosmological (at far distances). On the other hand, the majority of the models were indicating that the events of GRBs closer to the Earth (galactic origin) apparently to overcome the energy out put. During the era, the detection and interpretation of GRBs were not progressive due to lack of improved detecting instruments ,however GRBs as new field of science was opened at the end of the

era[?][?].

1.2.2 BATSE era (1991-2000)

The Burst And Transient Source Experiment (BATSE) was the early advanced space detecting instruments that carried on the Compton Gamma-Ray Observatory (CGRO), that capable to map Gamma-ray sources from almost the entire sky in energy range of (20keV - 2MeV). Between 1991 and 2000, BATSE detected 2704 GRBs, as shown in the diagram below. It can be seen that they are fairly uniformly spread over the entire sky, indicating that they are either nearby and clustered around our position, or they do not originate in our Galaxy. The contributions of BATSE in its nine years successful operations were:

- At its early operation in 1991, the apparent isotropic spatial distributions of 2704 GRBs were confirmed (see fig 1.2), and then the cosmological origin of GRBs was accepted by astronomers although the debate between galactic and cosmological origin continued until BeppoSAX. [?][?].

The fig below shows that the distribution is « isotropic »: the bursts are distributed randomly on the map indicating that they are either very close to the Earth, or very far, of extra galactic origin. No concentration of bursts along the plane of the Milky Way, symbolized on the map by the horizontal center line, appears. This most likely excludes candidates from our galaxy.

Long duration, bright bursts are shown in red, while shorter, weak bursts appear in purple. The bursts in grey are those for which the fluence could not be calculated, because of incomplete data. (The fluence indicates the total energy passing through a unit area; in X-ray astronomy, the unit of fluence is erg cm^{-2} .)

- Fireball model as the theoretical tool to explain the huge amount of energy driven from observed flux and fast time variability.
- confirm the classification GRBs into two types (short and long GRBs) according to bimodal distribution of duration parameter T_{90} .
- provide database of GRBs, their spectral and temporal properties [?][?].

limitations of BATSE

- unable to classify diversities (single spikey pulses, smooth with or multiple peaks, very

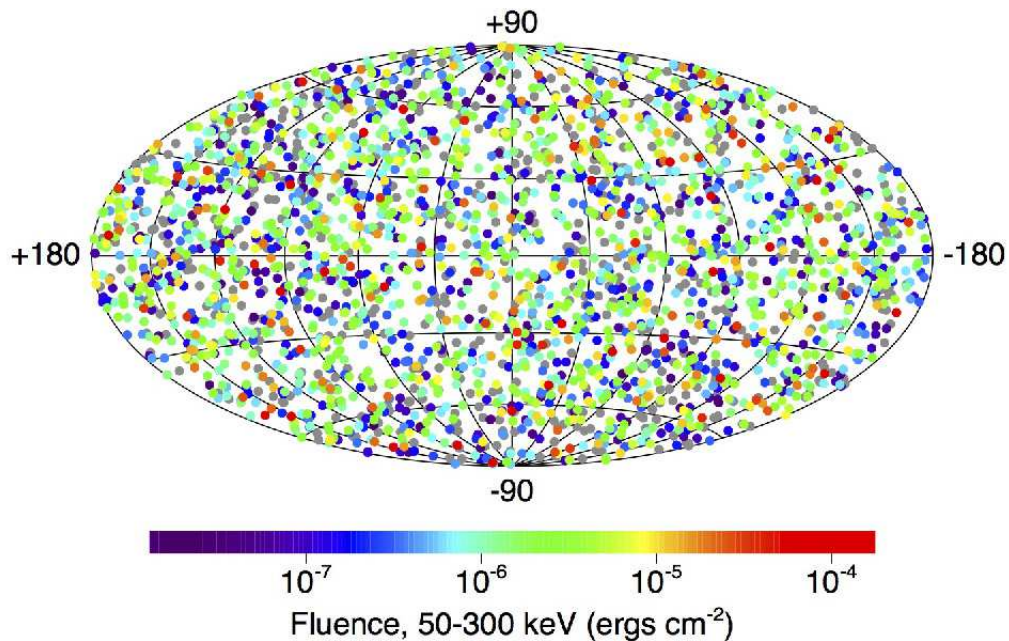


Figure 1.2: The distribution of all 2704 GRBs detected by BATSE satellite: they are clearly isotropic distribution . [?].

erratic, chaotic and spiky).

- BATSE's observations remain limited to gamma-rays alone, no follow-up observations at other longer wavelengths [?][?] [?].

1.2.3 BeppoSAX era (1997-2000)

BeppoSAX equipped with improved instruments on satellite launched in 1997. It was designed to detect long -living afterglows from X-ray to radio wavelength. In 1997, BeppoSAX detected the first X-ray afterglow within a GRB error box (GRB970228). An optical transient was also found, fading within a week (HST press release). The identification of GRB970228 with a host galaxy at a known distance (red shift of 0.695) confirmed the cosmological origin of GRBs. The contributions of BATSE in its seven years operations were:

- confirm the precise location of the burst in the X-rays rapidly transmitted and also discovered weak and decreasing signals. This was the late-time, weaker emission radiates in the X-rays, optical and radio waves.
- Opened a new era for the current understanding mysteries of GRBs.
- predicted the existence of GRBs afterglow in longer energy bands (from optical to radio wave length).

- Provide clues for GRB-SN possible connection , which was latter confirmed by HETE-2 and Swift that support collapsar model and explosions of massive star of wolf-Rayet (WR),leaving behind BH.
- Provide crucial information on the progenitors of GRBs.
- X-ray flash as new class of GRB with less-lumineous and low redshift identified from traditional GRBs [?] [?].

limitation of Beppo-sax

- unable to show the canonical behavior of x-ray afterglow which was later shown by swift [?].

1.2.4 Swift era(2004-now)

Before the launch of Swift, only longer bursts have been investigated, since commands had to be sent to the relevant satellite to point it in the correct direction, which this takes time. Swift is designed to be much more autonomous and, when it has detected gamma-rays, automatically slews to the position of the GRB within seconds.

Although the initial emission appears at gamma-ray energies, many bursts are also detected in the X-ray, optical and radio bands - the so-called afterglow emission. Swift is a multi-wavelength mission, with three instruments on-board - the BAT (Burst Alert Telescope), XRT (X-ray Telescope) and UVOT (Ultraviolet and Optical Telescope) - enabling the study of the initial burst and afterglow emission over a broad range of wavelengths. After a GRB has been detected and localized, follow-up observations with ground-based telescopes can occur. Among these are included the Faulkes and Liverpool robotic telescopes.

The Swift was a robotic spacecraft. It was launched into orbit on November 20, 2004 and orbits at 567 km x 585 km with a period of 95.9 min.is to investigate four phenomena : GRB progenitors, different physical processes underlying different GRB class observations, the interaction between the blast wave and its surroundings, and the early Universe through GRBs. Swift also aimed to investigates other non-GRB-related phenomena. It was the first multi wavelength mission for the study of GRBs, being elaborated by an international collaboration.In its ten years operations , Swift detected more than 2300 GRBs [?] [?].

Swift designed to detect and study the two phases of GRBs : prompt and afterglow emissions , and equipped with three sophisticated detecting instruments working together to observe GRBs and their afterglows in the gamma-ray, X-ray, ultraviolet and Optical wavebands.(see fig 1.3) The instruments and their functions described below:[?] [?]].

Burst Alert Telescope (BAT).

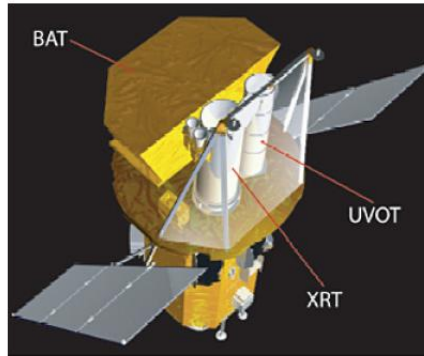


Figure 1.3: Schematic view of the swift satellite(Gehrels et.al 2004).The size of Mask of BAT is $2.7m^2$ [?]]

BAT detects GRB event and computes its coordinate (position) in the sky and locates the position of each event with an accuracy of 1 - 4 arcminutes with in 15 seconds. This position immediately relayed to the ground and rapid slew-ground based telescope catches the informations.

X-Ray Telscope (XRT)

It takes image and perform spectral analysis of the GRB afterglow. This provides more precise position of GRB with a typical error circle of approximation 2 arcseconds radius. The XRT also used to perform long term monitoring of GRB afterglow light curves and operated in energy range of 0.2 keV - 10 keV .

Ultra Violet optical Telescope (UVOT)

UVOT used to detect optical afterglow and provide a sub-arc seconds position. It also used to provide longer wave length follow ups of GRB afterglow light curves. Swift has been a great success in its observations. results include:

- Revealed unusual yet “canonical” X-ray afterglow behavior of X-ray flaring activity during the afterglow phase.
- show the transition from prompt to afterglow emission.

Finally, it detected the high- z GRBs such as 050904, 080913 and 090423, which were the most distant cosmic explosions [?] [?].

1.2.5 Fermi era (2008-now)

Fermi designed to focus on prompt emissions phase of GRBs by using much higher energy ranges (8keV - 300keV) than swift (15keV -150keV). It carries on board two types of detectors known to be Gamma-Ray Burst Monitor (GRBM) and Large Area Telescope (LAT). They provide unprecedented spectral coverage for seven orders of magnitudes of energy from 8 keV to 300 GeV. Fermi made Significant progresses for the current understanding of origin of GRBs.

The contributions of Fermi since launched were:

- The existence of three elemental spectral components (Band function-like, thermal and extra non-thermal power-law component) in GRB spectra was confirmed.
- Suggest that the featureless Band function spectra extended from keV to GeV band a Poynting-flux-dominated flow.
- Explain the existence of thermal components in some GRBs(e.g GRB 5090902B) due to hot fireball without strong magnetization.
- The delayed onset of GeV emission in some LAT GRBs suggests that there likely be a change of either particle acceleration condition or the opacity of the fireball during the early prompt emission epoch.
- confirms that long lived GeV emission is likely of external origin, while GeV emission during the prompt phase, on the other hand is likely of internal origin [?] [?].

1.3 Classification of gamma-ray bursts

Based on the bimodal distributions of duration T_{90} or T_{50} of prompt phase or hardness ratio , GRBs have been catagorized in to two groups: short/hard and long/soft GRBs. The duration of GRB, T_{90} or T_{50} , is defined by the time interval over which 90 % or 50 % of the burst fluence is detected respectively. The typical duration of a GRBs is $\sim 20 - 30$ seconds for long bursts and $\sim 0.2 - 1.3$ seconds for short one. Observational result tells us that the duration of GRBs can be in a range of 5 orders of magnitude, i.e, from $\sim 10^{-2}$ s to $\sim 10^3$ s. The bimodal distribution of T_{90} has been used to identify the two categories of GRBs, namely, “long” or “soft” (T_{90}

≥ 2 s) and “short” or “hard” ($T_{90} \leq 2$ s) (see Fig1.4). Instrumentally , T_{90} or T_{50} depends on the energy band and the sensitivity limit of the detector. Theoretically,

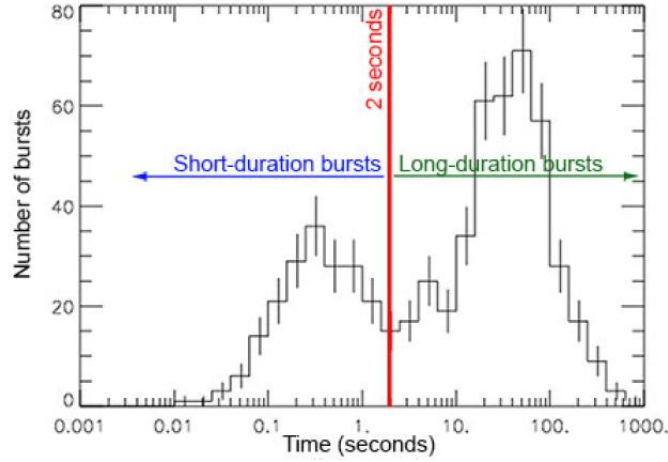


Figure 1.4: The GRB classification (long and short) distribution. GRBs last between a few milliseconds and several minutes. There appear to be two populations, ‘short’ bursts, with duration peaking around 0.3 seconds and ‘long’ bursts, which last around 30 seconds, with the ‘dividing line’ between the groups being 2 seconds.

there are three timescales which may be related to the observed GRB duration T_{90} :

- (1) central engine activity time scale t_{eng}
- (2) relativistic jet launching time scale t_{jet}
- (3) energy dissipation time scale t_{dis} . Then, the observed GRBs duration T_{90} should satisfy: [?]

$$T_{90} \leq \delta t_{dis} \leq \delta t_{jet} \leq \delta t_{eng} \quad (1.1)$$

1.3.1 short/hard gamma-ray bursts

Short/Hard gamma ray bursts (SGRBs) are events with a duration T_{90} less than 2 seconds and account for about 30% of the total gamma ray bursts. They are highly energetic /hard gamma-rays when compared with their long burst counterparts. For many years short-hard GRBs were not deeply researched as long GRBs. As a result, study of short-hard GRBs (SHBs) limited. However, one year after swift launch, in 2005 a breakthrough occurred following the first detections of SHB afterglows [?][?].

The swift observations established that SHBs are cosmological relativistic sources that, unlike long GRBs, do not originate from the collapse of massive stars, and therefore constitute a distinct physical phenomenon. One viable model for SHB

origin is the coalescence of compact binary systems , in which case SHBs are the electromagnetic counterparts of strong gravitational-wave sources. In this burst, the conversion of energy into gamma- rays decreases as the burst progresses. There is no radio, optical, or x-ray counterpart has found for any short burst [?].

1.3.2 long/soft gamma-ray bursts

Another subclass of GRBs that account for 70% and have a duration of greater than 2 seconds are classified as long/soft GRBs (see fig 1.4 above). All long bursts display x-ray afterglow and about one-half as radio or optical afterglows. In long duration bursts energy conversion appears to remain constant through burst. Their creation linked to a young galaxies with rapid star formation and to a core collapse of supernova as well. This is unambiguously associating long GRB with the death of massive stars. Observations of LGRB afterglow at high red shift , are also consistent with the GRB having originated in star-forming regions [?].

1.3.3 Ultra long gamma-ray bursts (ULGRBs)

GRBs with highly a typical duration of more than 10,000 sec called ultra-long gamma-ray bursts (ulGRBs). They are the tail end of the standard long GRBs that caused by the collapse of a blue supergiant star, tidal disruption events or a new born magnetar. They have been proposed to form a new third class of GRBs. One explanation which has been proposed for their ultra-long duration is that they could have progenitors differ from classical GRBs in that: they could be produced either by the core collapse of a low-metallicity supergiant blue star, the birth of a magnetar following the collapse of a massive star or the collapse of a Pop III star. In any case, it is clear that the duration of these bursts make them so peculiar that they need further studies [?] [?].

1.4 Global properties of GRBs

Two distinct global properties of “classical GRBs” began to emerge—the intensity /brightness and the angular / location distributions—both are important implications for the distance scale of GRBs and hence their origin.

1.4.1 Intensity distribution

The brightness distribution of GRBs appeared to show that we were seeing out to the edge of the GRB population: there were too few faint GRBs relative to the

number expected if GRBs were uniformly (“homogeneously”) distributed in space. Brightness was most straight forwardly measured as the peak flux (P , with units $[\text{erg s}^{-1} \text{ cm}^{-2}]$) in the light curve of a GRB. The brightness distribution is usually measured as the number, $N(>P)$, of GRBs brighter than some peak flux P per year. If the peak luminosity (L , with units $[\text{erg s}^{-1}]$) of all GRBs is the same, then, using the $\frac{1}{r^2}$ law, for a given flux P we would see all the GRBs within a maximum distance: [?] [?].

$$d_{max} \approx \sqrt{\frac{L}{4\pi P}} \propto P^{-\frac{1}{2}}$$

All the GRBs to that distance would be brighter than P by construction. The number of GRBs we would detect to that brightness (or brighter) in one year would just be the volume times the intrinsic rate (R , in units of $[\text{event yr}^{-1} \text{ per volume element}]$): $N(>P) \propto V \times R \propto R \times d_{max} \propto R \times P^{-\frac{3}{2}}$. So with a homogeneous distribution, we expect that the number of faint GRBs N should grow as a power law proportional to $P^{-\frac{3}{2}}$, where the constant of proportionality scales directly related to the intrinsic rate R : for every ten times fainter in flux we observe, we would nominally expect about thirty-two times more GRBs. While this was indeed seen for the brightest events, there was a flattening at the faint end of the brightness distribution. This flattening was highly suggestive that we were seeing the “edge” of the GRB distribution in space, an important clue in understanding the distance scale. But without knowing the intrinsic luminosity L , we could only infer the shape of the distribution, not the scale. It was like seeing a picture of a building but not knowing if it was of a miniature in a snow globe or the life-sized version [?] [?].

1.4.2 Angular distribution

The locations of GRBs on the sky appeared to be randomly (isotropically) distributed: that is, there was no indication that any one direction on the sky was especially more apt to produce GRBs than any other (see fig1.2 in section 1.1). If GRBs were due to neutron stars strewn through out the disk of the Galaxy, for instance, the locations of GRBs on the sky should have been preferentially located near the Galactic plane (as is seen with SGRs). If associated with older stars in the roughly spherical “bulge” of the Milky Way, GRBs would have been preferentially located in the direction toward the Galactic center and less so toward the opposite direction.

The inference that the Sun was roughly at the center of the GRB distribution in space, while casting aside some models, still allowed for a variety of distance scales: from a fraction of a light year to billions of light years [?].

1.5 Statement of the problems

As mentioned in section 1.1 above, to study the mystery and phenomenology of Gamma-ray bursts, several satellites (from Vela at early time to Fermi and others at recent time) equipped with different instruments (telescopes) have been launched. Among those satellites, Swift was open new era for the current understanding and development of gamma ray researches. Swift missions detected prompt and afterglow emission phases of gamma-ray burst. Not only this, the temporal and spectral behaviors, Light curve properties of x-ray and optical afterglow of gamma-ray burst also studied in detailed. However, as far as my search /review literature is concerned, there is knowledge gaps explaining more about canonical x-ray afterglow light curves:

- Does x-ray afterglow results of internal or external shocks ?
- What parameters / variables responsible for the variations of temporal and spectral indices of canonical x-ray ;
- what is the implications variations both indices.

In this thesis, I emphasized on the theoretical and observational properties of canonical X-ray afterglow light curves qualitatively and quantitatively.

Regarding this work the unclear ideas or un answered questions are listed below. Among these:

- (1) what are the cause of canonical x-ray light curve of afterglow gamma-ray bursts?
- (2) what are the progenitors of canonical x-ray light curves?
- (3) Did the value of temporal index of any random GRB confirmed to the proposed value in all phases canonical x-ray light curves?
- (4) Could some of the breaks at end of the plateau phase actually be jet break or late steep decay phase? The goal of this thesis is attempt to explain and give answers for these questions.

1.6 Objectives and thesis outline

General objective

To study how characteristic of light curves gamma ray bursts affected by some

parameters or variables such as flux ,luminosity and time.

specific objectives

- To explain the cause and effect for the variations of light curves of prompt and afterglow phases.
- To compare / contrast the proposed values of temporal and spectral indices of x-ray afterglow with/to the calculated values.
- To describe the implications of temporal (α) and spectral (β) indices gamma -ray afterglows.

Thesis outline

Hereafter, I point out the outline of the thesis. In chapter 1 above, the background of gamma -ray physics and a short historical discoveries /explorations/, gamma-ray burst as well as gradual development of them for the past five decades would be discussed. In chapter 2 , I intended to explain the emission mechanisms of both phases of GRBs as well as their theoretical and observational properties using standard fireball models. Furthermore , the canonical properties of x-ray afterglow ,decaying of x-ray flux with time and its intensity discussed deeply.

In chapter 3, I address methodology and methods , models and tools used to analyze the temporal and spectral properties of canonical x-ray light curves in swift/XRT for some selected gamma-ray bursts with specified red shifts and have two or more light curve breaks. In chapter 4, I discuss on achieved results / findings comparing /contrasting with proposed values using tables and figures . Finally, I put a brief summary or review of the enlightenment of this work , and forward suggestion on unexplored area of the field for future research in the last chapter.

Emission mechanisms and observational properties of gamma-ray bursts

Introduction

This chapter comprises eight sections that related to each other to explain gamma - ray physics. Overall , the phenomenology of gamma - ray burst: emission mechanisms of gamma-ray bursts, observational properties of gamma-ray bursts (prompt and afterglow phases), interpretation of gamma-ray afterglow especially x-ray afterglow , decaying of flux with time are discussed accordingly. Finally flux (F) and light curve intensity (f) are defined and their equations are also derived briefly.

2.1 GRBs production mechanisms

GRB emission mechanisms:- are the theories or models that visualize or explain how the energy from GRBs progenitor (sources) is turned to radiation. In the early 1990's more than 100 potential models were developed to describe the phenomenon of GRBs. However, more constraining observations over the years have resulted in the development of a standard model called " Fireball model " to describe well about the emission mechanisms of GRBs and their afterglow , properties of GRBs progenitors. It was a neat theoretical standard model that has been revised that attempt to explain the mysterious events of GRBs for a longer time.[?]

2.1.1 Basic fireball model

Gamma-Ray Bursts (GRBs) are the most energetic events in the universe. During GRBs (the most powerful bursts) impressively can eject energy equal to over 9000 supernovae. These energy levels are so extreme that they cannot be created by thermal processes. So, what causes these high energy levels? The Fireball Model

is one of the few models that has been put forth to explain why GRBs tend to have such high energy levels. It also attempts to explain the time scales that govern the phenomenology of prompt and afterglow phases. [?] [?].

The variability of GRBs light curves directly related to the high energy levels, as the variability indicates that it occurs over a very small area with the emission of GRB energy being in the order of 10^{52} ergs, coming from a very small volume of space with highly concentration of radiation energy, and then theorized that a Lorentz factor of $\Gamma \sim 100$ be associated with the GRB. In short, the fireball model must be able to encompass all of these variables in order to apply to all GRBs (and thus be a plausible model to study GRB physics.[?].

The name of the fireball model suggests the mechanism to which a GRB occurs in a fireball of ultra-relativistic energy consisting of optically thin material with very few baryons. In essence, during the GRB event, the inner engine remains undetectable due to the optical thickness and the lack of a thermal profile due to the compactness problem. The highly relativistic expansion of fireball overcome the compactness problem and can cause the internal shocks that produce the detectable GRB, while the external shocks form the gradual afterglow [?].

The first relativistic fireball model was proposed by (Paczynske 1986, Goodman 1986). They had shown that the sudden release of a large quantity of gamma ray photons into a compact region can lead to an opaque photon-lepton “fireball” through the production of electron-positron pairs e^-e^+ . The most fundamental property the fireball can be characterized by its initial energy E_o . In the fireball there are M_o baryons (electrons have negligible mass) with $M_o \ll \frac{E_o}{c^2}$, and its mean energy per baryon, $\eta = \frac{E_o}{M_o c^2}$ [?] [?].

Fireball model predicted that when the expanding plasma becomes optically thin, and hence the emitted radiation escapes within created burst. This mechanism would generate a quasi-thermal spectrum rather than the observed power-law spectra, thus indicating the difficulty inherent to explaining the duration of the GRB having such a small timescale (just a few seconds). Moreover, the fireball baryonic load is another model which converts all its energy into kinetic energy rather than into luminosity to produce a quasi-thermal spectrum. This model, however, does not explain the efficient emissions of radiation. In particular, the

origin of the emission associated with the two phases is produced by two different mechanisms: a matter-dominated, and a radiation-dominated. The assumption that the fireball is matter-dominated is widely used, and which consists of baryons, electrons and positrons, and photons resulting from the merger of binary neutron stars or a collapse of massive stars [?] [?] (see fig 2.1).

The emitted energy is higher than the mass of the baryon in the rest frame

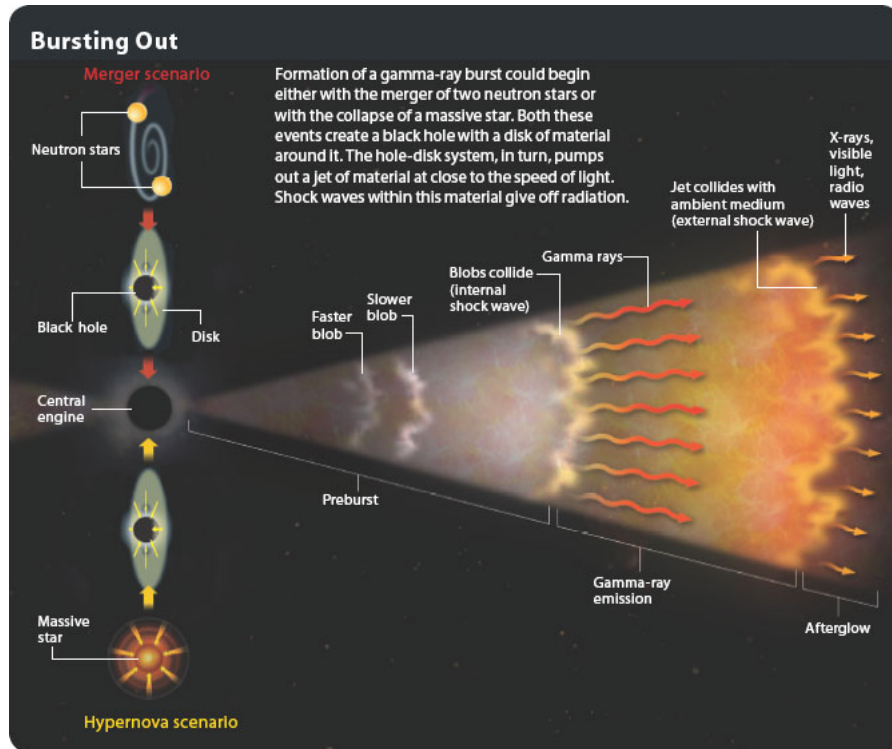


Figure 2.1: Visualization of the fireball model that illustrates the various steps of basic standard model with the internal and external shocks and radiations. At the left the two main scenarios (collapser and merger) indicated that they lead to a central black hole surrounded by a disk. (from Gehrels et al. (2002), credit Juan Velasco)[?]

by a factor of ~ 100 , with the baryon accelerated with in an expanding fireball to a higher Lorentz factor, Γ . During this process, two major out comes can be seen: at the photosphere, a fraction of the thermal energy is radiated away and the accelerated electrons produce a non-thermal gamma ray spectrum by a synchrotron or an IC processes in the internal shock at large jet radius. Rather, the outflows that formed from the central engine are believed to be dominated by Poynting flux [?] [?].

The shocks in the fireball model are collisionless, whereby the particles involved

are accelerated and scattered within the Fermi process when crossing the shock interaction. This can result in the type of energy distribution that can be described by a power law ($\alpha \sim 2 - 3$). In such a situation, the electrons emit a non-thermal radiation of photons via two different mechanisms, synchrotron and Inverse Compton scattering, that extend to very high energy (GeV bands). [?] [?].

Dissipative process

Dissipative process :- is the of outflows or shock waves from central engine interact with interstellar medium (ISM) to produce both GRBs and its afterglow - the external and internal shock models, that successfully interpret the prompt and afterglow emissions respectively. In particular, the origin of the emissions associated with the two phases is produced by two different processes. [?] [?].

Internal shock model

The internal shocks are the mechanism for the production of the observed highly energetic gamma-rays. Moments after the initial GRB event, shock waves emanate from the inner engine at relativistic speeds [99.995% of the speed of light at a Lorentz factor of ~ 100 . The fireball is dynamic; it isn't just one shock wave emanating from the compact source. Instead, different shock waves will be traveling at different relativistic speeds, and it is the interaction between these different shock fronts that cause the energetic gamma-ray emissions [?] [?].

The internal shocks traveling at relativistic speeds convert kinetic energy into gamma-ray photons, this is the only way to get high energy gamma-rays that are observed (as previously mentioned, they cannot be emitted through a thermal process). When internal shocks interact with each other as they are moving at relativistic speeds, the interactions produce Inverse Compton and Synchrotron emissions [?] (see fig2.2).

Initially, the fireball is optically thick but as it expands and cools it becomes optically thin, allowing the gamma-ray photons to escape. Early models had the fireball and the internal shock waves as being purely radiative, but this didn't follow what was being observed (it would have made a profile too smooth). To solve this problem, some baryonic mass was added. This allowed for the internal shocks to become effectively contaminated. The added baryonic mass also aids in the conversion of some radiation energy into kinetic energy, which helps with

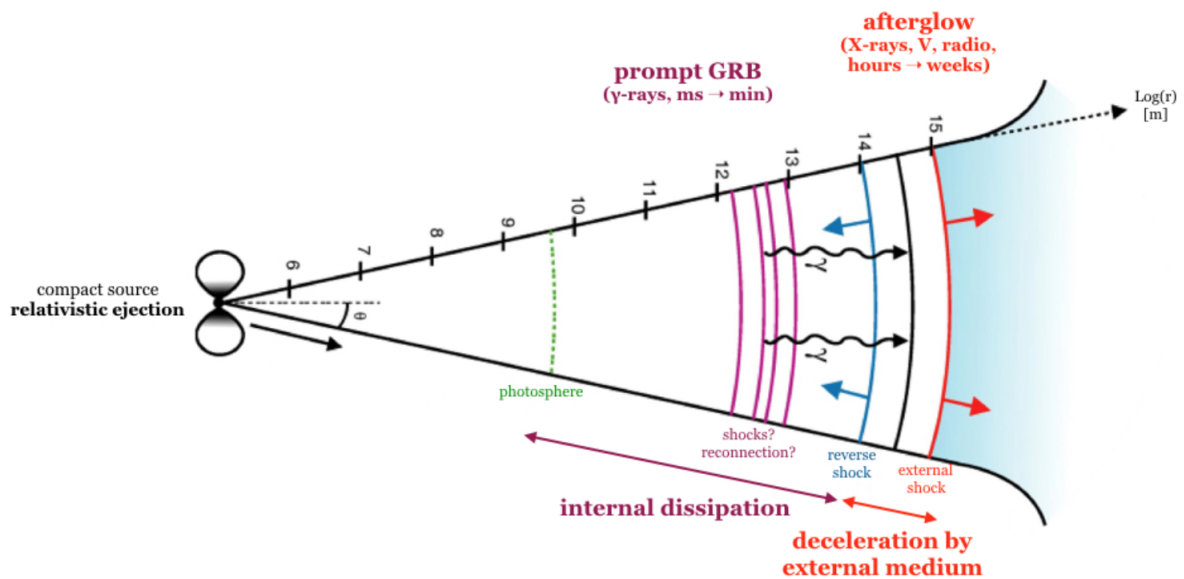


Figure 2.2: Standard fireball model.

an added kick to the relativistic kinetic energy of the shock waves, this in turn increases the gamma-ray energy more. Even if all of the shock waves emanate from the core at the same speed they will eventually cross over multiple times. As the shells are emitting through inverse Compton, it is slowing the shock front, thus increasing the times that many shock waves interact with one another. The earlier shock waves are likely to be emitted slower than the later emitted shock waves, this would also increase the amount of interactivity between the different shock waves. [?] [?]].

External shock model

The external shock waves are used to explain the afterglow that was first detected by BeppoSAX in 1997, as the internal shock waves are not able to explain the duration of the afterglow nor the wavelengths that are detected (which range from soft x-ray through to radio). The name can be a little misleading at first; the external waves actually refer to the internal waves at a later stage –once they’ve cooled down and continue emanating from the source. As the shock waves continue out they will eventually interact with the Interstellar Medium [ISM] (such as a molecular cloud or some other impedance), and it is the shock waves’ interaction with the dust/gas that cause the afterglow. Unlike the internal shocks, the external shocks are primarily a thermal emission (see fig 2.3). The energy transferred from the shock waves is deposited into the ISM; this material can then be caught up in

the shock front and emit radiation. As the shock waves began with a lot of energy, there is a lot that can be deposited into the ISM, this is what can cause such long afterglow and why it covers all parts of the energy spectrum [?].

A relativistic materials/jets are running into some external ambient medium i.e

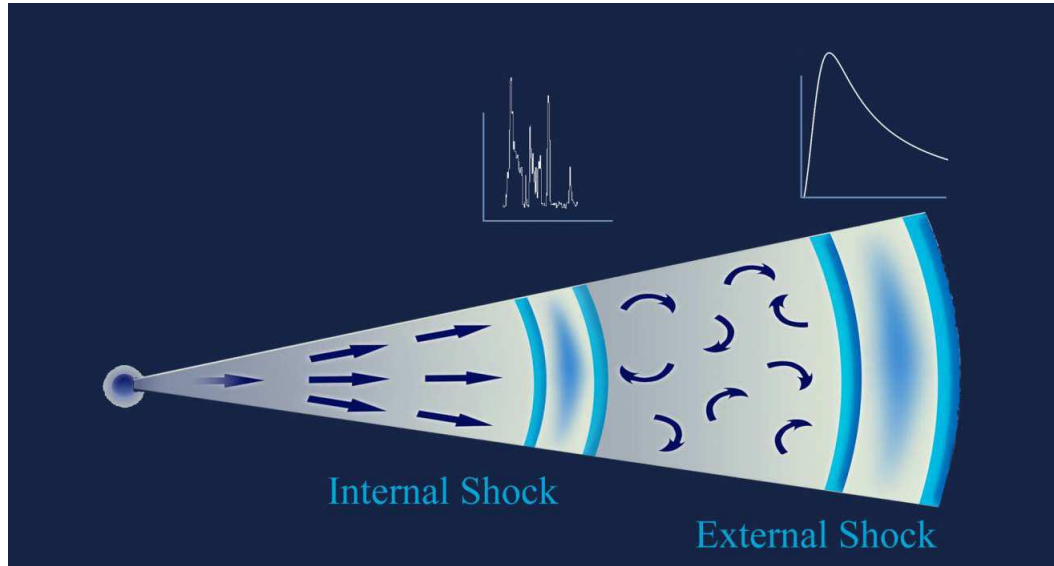


Figure 2.3: Qualitative schematic view of the structure of the relativistic jet produced by the gamma-ray burst. The external shock arises as a result of the impact of the jet on the stellar wind of the progenitor. This is where the final goodbye of the SOS similar emission from the collapsing star forms, which is characterized by a smooth (but non-monotonic) light variation. The internal shock persists as long as the central engine continues operating this is where rapidly varying gamma-, x-ray, and optical radiation forms.

interstellar medium or stellar wind. In each time, the ejecta run a high density environment in which they produced a peak in the mission called external shock [38]. In the external shocks, the jets may be forward shocked or reverse shocked. As the material in the jet expands, accelerates and compresses interstellar medium, It creates a forward shocks. The deceleration of forward shocks is occurred when the rest mass energy of the swept up particles equal to the ejected energy. This sets a deceleration length scale at ($\sim 10^{16}$ cm) . The reverse shock is formed by the deceleration of the jet material and propagates back into the relativistic flow. This happens when the rest mass energy of the swept up particles is greater than the ejected energy [?].

Although it would be correct to assume that all GRBs have an external shock,

about half of detected GRBs don't have a detectable afterglow. The reason that no afterglow being detected is not thought to be the exposures aren't long enough, or because we're observing too early or too late. Rather, GRBs occur in high mass systems, whether it be through a supernova or NS-NS and NS-BH merges, this means that they had very short stellar lives and may still be inside of a molecular cloud. Molecular clouds are very optically thick environments so the reason we're not able to detect the afterglow in about 50% of the time could just be due to reddening, absorption, or scattering.

Radiative process

Synchrotron Radiation

Synchrotron emission is the non-thermal radiation produced when a relativistic electron gyrates in a uniform magnetic field. Synchrotron radiation can explain the GRB prompt emissions, and is considered to be one of the more important mechanisms in various astrophysical phenomena. The synchrotron shock mechanism, which is produced by the optically thin plasma in a weak magnetic field, can be used to predict the form of the observed spectra [1] [2] [3] .

Synchrotron emission can be classified as having two regimes: the "fast-cooling" phase, which describes when the timescale for the cooling of the electrons is shorter than the dynamical lifetime of the source, resulting in an electron that cools quickly compared to the low-level injection of energy; conversely, "slow-cooling" occurs when the timescale for the cooling of the electrons is longer than the dynamical lifetime of the source . The differences between these two regimes are associated with the emission's radiative timescale [4] [5] .

The peak frequency, the cooling frequency, and the self-absorption frequencies set the characteristic break frequencies in the synchrotron spectra. These frequencies evolve with time; indeed, their evolution is reflected in the complexities observed in the shapes of the light curves at certain band energies . This model can successfully describe the afterglow. Thus, the optically thin synchrotron spectrum is currently considered the best spectral fitting model for most GRBs. The first synchrotron model was applied to the spectral fitting of GRBs by Tavani (1996), and subsequently by Baring and Braby (2004) [6] [7] .

Synchrotron Self-Compton

Inelastic collisions between low-energy photons and ultra-relativistic electrons are known as the IC processes. Each astrophysical source has an Synchrotron Self-Compton (SSC) scattering component when synchrotron radiation that energizes it provides the means to scatter its seed photons to high energies and across a large frequency range. Thus, the phenomenon responsible for creating high-energy emissions from GRBs and other astrophysical sources is accepted to be the SSC mechanism. The SSC mechanism, while complex, uses a simple power-law function to explain the injected electron spectrum. The SSC spectrum can be described precisely as carrying out a complicated seed photon spectrum convolution and electron energy distribution. In certain circumstances, the GRB spectrum can be modelled as an SSC component at very high energy ~ 10 MeV.[?][?]

2.1.2 GRBs progenitors models

There are three ways to produce lots of energy in nature: nuclear, gravitational, and rotational. The nuclear energy does not have enough efficiency to power a GRB. For example, the proton-proton chain that is responsible for energy production in stars has an efficiency of about 0.0067. The gravitational potential energy released during a collapse of a massive star or during the merger of two stars has enough energy to power a GRB. The rotational energy from a black hole also may be enough to power a GRB. It is also possible that both of these last two mechanisms play a role in GRB energy release. The central engine that produces the initial energy, E_o , is hidden from direct observation. However, the observed temporal structure is thought to reflect the central engine activity. The central engine must satisfy the following general features:

- Capable of producing an extremely relativistic energy flow containing $\approx 10^{51}$ - 10^{55} erg.
- Highly variable flow resulting in highly variable light curves.
- Activity can last from a fraction of a second to a few hours.
- Possibility of late time activity that may cause X-ray flares.
- Relatively rare event as suggested by observed GRB rates.

2.1.3 Working mechanisms of central engine

The central engine is of great importance, as it needs to be able to push material out very near the speed of light. The inner engine of a GRB is a highly compact source, and it is the highly compact nature of this object that leads to the idea that

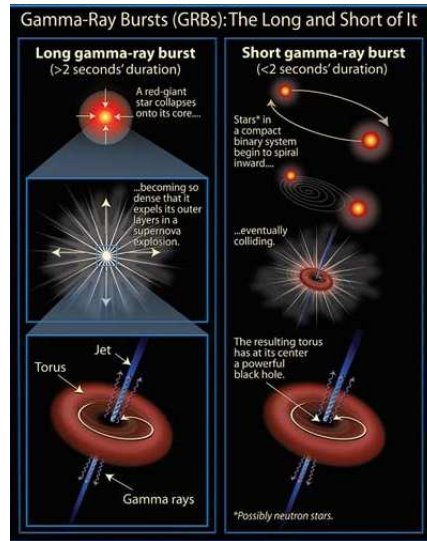


Figure 2.4: Schematic scenarios for plausible progenitors of long and short GRB. The exact nature of the GRB progenitors is unknown, although it is possible that long GRBs come from the collapse of massive, rapidly rotating stars and short GRBs result from the merger of compact objects.

[222]

the core of the inner engine of a GRB is either a neutron star or a black hole (as they're the two most compact sources that we're currently aware of) The workings of this inner engine will alter depending on whether it is a long or short GRB being observed. A short GRB has been thought as occurring during a neutron star binary collision [NS-NS] or a neutron star-black hole collision [NS-BH]. It has been suggested that a long GRB could be associated with a hypernova – a Wolf-Rayet type star undergoing a core collapse supernova.[?]

2.1.4 GRB-SN association

2.2 GRBs Observations and interpretations

GRBs composed of two main radiative phases: the prompt and afterglow phases. The former typically observed in soft gamma-ray (10 keV to 10 MeV), and generally lasts between $\sim 100\text{ms}$ and $\sim 1000\text{ s}$, although there is a wide variety of different temporal behaviors observed, from single pulses to complex temporal evolution. The spectrum of this prompt emission is non-thermal, often described by a Band function with a typical peak around $\sim 200\text{ keV}$. The afterglow emission is most often detected from X-rays to radio waves and fades with time. In the optical, the temporal fading goes typically as t^{-1} , however the slope of this fading depends on

the wavelength and on the burst. This means an afterglow observed in the optical will frequently fade beyond the reach of most ground-based telescopes within a week. In the radio however, there is evidence of emission from the afterglow up to a few months or even years after the burst. The sudden flash of gamma rays emitted in the creation of a GRB was the route by which GRBs were detected and the property for which they are named. The prompt emission is readily detected, even by rudimentary space-based gamma-ray detectors, due to the extreme high-energy photon budget that GRBs exhibit. Indeed, at peak, GRBs outshine all other sources within gamma-ray sky, including the Sun.[?]

2.2.1 prompt GRB emission

prompt emission of GRBs is defined as the emission observed during the gamma-/hard X-rays phase, whose photons are the ones triggering the space instrumentation leading to multi-wavelength follow-up observations. It is believed to be the direct outflow ejected from the central engine; as per the "fireball" model, which deposits its gravitational energy into a thermal explosion. In other words, the prompt emission occurs when the kinetic energy from a catastrophic explosion event, such as massive star core collapse or the merger of two compact stars, is converted into electromagnetic radiation due to the internal shocks that result from collisions between shells of ejecta.[?]

prompt emission generated due to internal shocks magnetic dissipation within the fireball take place effectively above the pair production photo sphere at 10^{12} to 10^{14} cm. These shocks splits from mini-shells within a jet produced by unsteady accretion of materials onto black hole or by the merger of binary neutron stars (BNS). The shells have a distribution in lorentz factor $\gamma \propto \Gamma$ where Γ is bulk lorentz factor.[?][?]

In the region around $\sim 10^{12}$ cm to 10^{14} cm , the collisions between different parts of the flow is produced in different shells (see fig 2.4 (a) and(b)). As a fast shell catch up with a slower ones, they form strong internal shocks that propagates in both shells with out deceleration. Once shell became above the photo sphere, the heated and accelerated electrons cool by synchrotron emission then radiation is observed in γ -ray band. Each collision that occurs above pair photo sphere produces a pulse in the GRB's light curves[?]

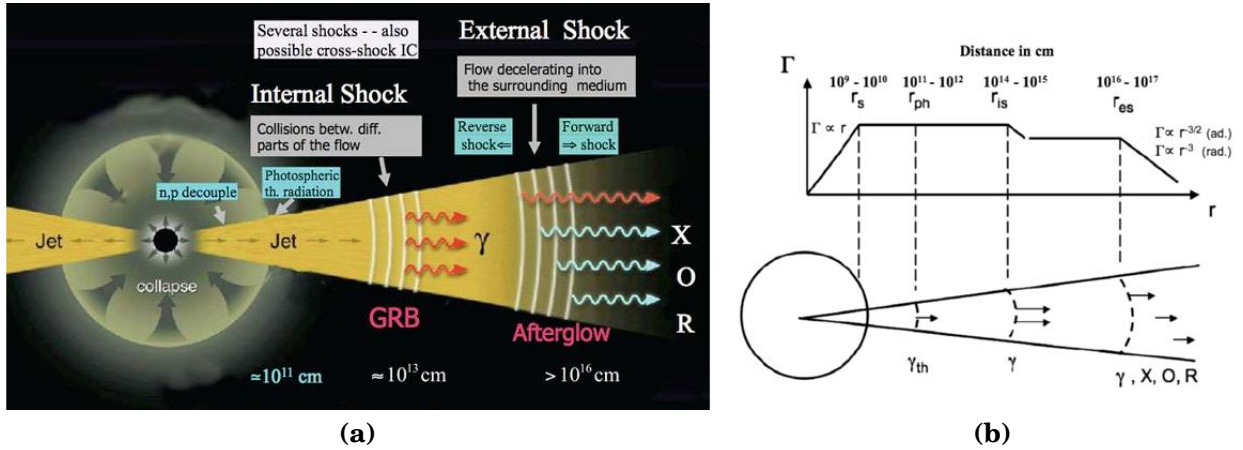


Figure 2.5: (a) Collapser model that show internal and external shocks producing prompt and afterglow emissions respectively. (b) Schematic evolution of the jet Lorentz factor and examples of symbolic locations of radius: the saturation radius r_s , photo spheric radius r_{ph} , internal shock radius r_{is} and external shock r_{es}

Thus, GRB light curves represent the count rates/photons recorded by the high energy detectors as a function of time. Each of the recorded events shows different variability patterns, meaning that each light curve is different from the rest. As it is shown in Figure 2.6, the light curves can be classified into four different categories Pe'er, 2015:

- single-peak events (e.g. GRB 910711),
- a smoothed light curve composed with several peaks (e.g. GRB 920221),
- separated multi-collisions (e.g. GRB 930131A),
- and irregular peaks (e.g. GRB 991216)

The result is that the fireball expands due to the effects of thermal pressure and is then accelerated to relativistic speeds, where the thermal energy is ultimately released in the form of photons at the photo sphere. In the internal shock case, the dissipation happens inside the ejecta, where the ejecta is decelerated by the surrounding medium and this deceleration happens after the internal shock phase ceased. [?][?][?]

2.2.2 Afterglow GRB emission

Afterglow is the phase of GRBs that slowly fading at longer wavelength. This emission is created by the collision between ejected bursts and the surrounding medium or interstellar gas or dust. The GRB itself is rapid, lasting from less than a second up to a few minute at most. Once it disappears, it leaves behind a counterpart at a longer wavelengths from X-ray to radio bands . Then, they

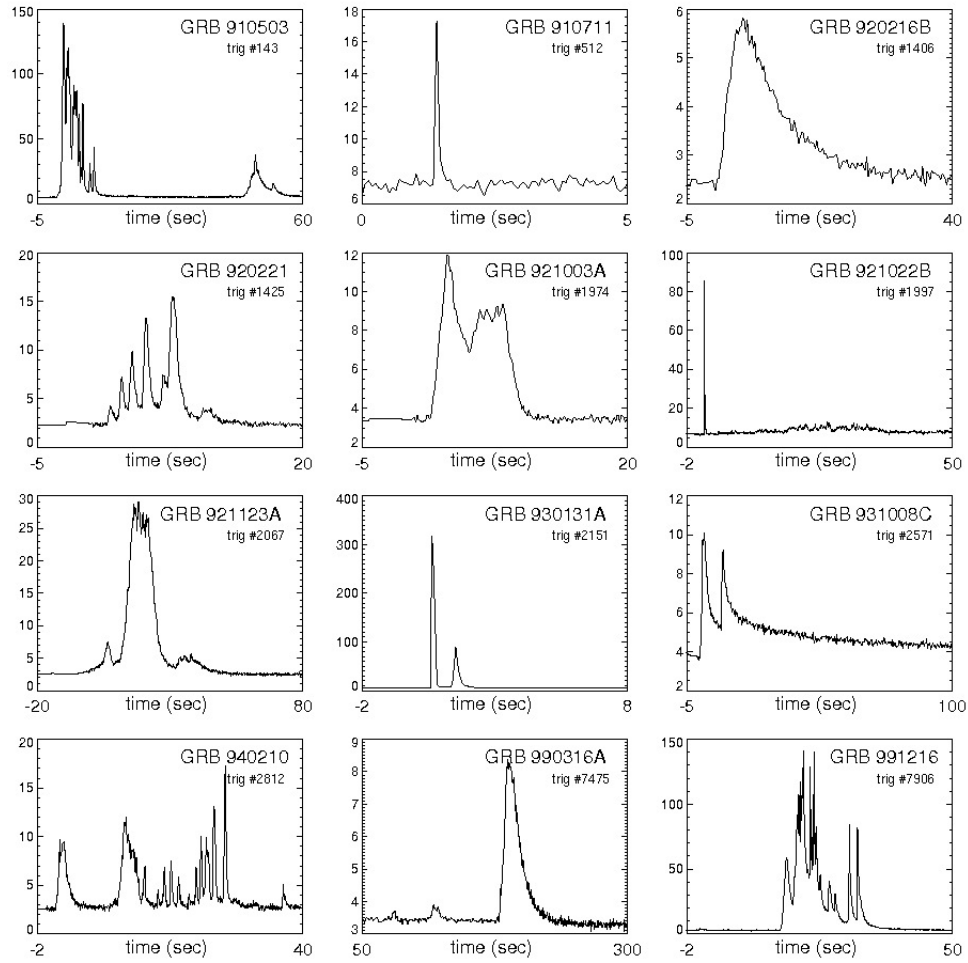


Figure 2.6: Diverse light curves of the GRBs prompt emission detected by BATSE instrument. This sample includes short and long events. <https://gammaray.nsstc.nasa.gov/batse/grb/lightcurve/>

[Firaol Fana]

are remain detectable for day or longer. As we have mentioned above, afterglow emissions are dominated by external shocks. Due to lack of advanced instrument, early searches were unsuccessful largely to observe the bursts' position at a longer wavelength immediately after the initial burst. Once the GRB faded deep imaging was able to identify a faint, distant host of galaxy at a location of GRB as pinpointed by the optical afterglow. [?] [?] [?]]

2.3 Interpretations of GRBs afterglow

Before launch of the Swift satellite, broad-band, late time ($t > \sim 10$ hours) afterglow data had been collected for a moderate sample of GRBs. These observations were generally consistent with predictions of the external forward shock, synchrotron

emission, model. The main observational properties of late time afterglow radiations are:

- In general the optical afterglow displays a power law decay behavior $F_\nu \propto t^{-\alpha}$, with a decay index $\alpha \sim 1$. This is consistent with the prediction of the standard external shock afterglow model.
- A temporal break in the optical afterglow light curve is usually detected for bright GRBs. The break time is typically around a day or so, which is followed by a steeper decay with slope $\alpha \sim 2$. This is consistent with the theoretical prediction of a “jet break”.
- The radio afterglow light curve initially rises and reaches a peak around 10 days, after which it starts to decline (e.g. Frail et al., 2000). The peak usually corresponds to passage of the synchrotron injection frequency ν_m , or the synchrotron self-absorption frequency ν_a , through the radio band.
- The broad-band afterglow spectrum can be fit with a broken power law, at a fixed observer time as one expects for the synchrotron afterglow model.
- For bursts with high-quality data richer features in the optical light curves have been discovered, which include bumps and wiggles that deviate from the simple afterglow model predictions. Smooth bumps in afterglow light curves with duration $\delta t_{obs} \sim t_{obs}$ may be interpreted as due to density bumps in the external medium where as sharper features in light curves might be due to energy injection from the central engine angular fluctuations in energy per unit solid angle [?].

2.3.1 Late time afterglows

Before swift mission, afterglow observations was started after several hours (10 hrs) after bursts trigger. The optical afterglow of late time displays a power law decay behavior $F_\nu \propto t^{-\alpha}$, with a decay index $\alpha \sim 1$. The temporal break in the optical afterglow light curve was detected for bright GRBs. The break time is typically around a day and followed by the steeper decay with decay slope of $\alpha \sim 2$ [?]

The radio afterglow light curve initially rises and reaches a peak around 10 days after starts to decline . The peak usually corresponds to the passage of synchrotron injection frequency ν_m or synchrotron self absorption frequency ν_a through the radio band. The broad band afterglow spectrum can be fit with a broken power law at a fixed observer time.[?]

2.4 Theoretical interpretation of X-ray afterglow

Afterglow gamma-ray bursts observed at all wavelengths such as: X-ray [?], optical [?], IR, and radio [?]. X-ray afterglow is the first and strongest, but shortest signal. In fact it seems to begin already while the GRB is going on. X-ray light curve observed several hours after the burst can usually be extrapolated to the late parts of the prompt emission. Due to its low variability and observed time range (from minutes to weeks after the GRB event), a canonical X-ray light-curve for the afterglow was defined from the result of Swift /BAT-XRT instruments. The four segments, with their corresponding temporal indices, are associated two by two and identified as early and late afterglows [?], [?] [?] : I and II (respectively the steep and shallow decay), and III and IV (respectively a standard afterglow and a jet break). Part I and III, marked by solid lines, are most common and the other two components, marked by dashed lines, are only observed in a fraction of all bursts. Part I, thought to be associated with the prompt phase when the central engine is still active; the rest of the afterglows are due to the dynamics of the interaction between the jet and the surrounding medium. [?] [?] [?] [?].

GRBs early afterglows detected within less than 100 seconds after trigger in the swift mission. The canonical X-ray afterglow light curve generally includes four phases such as early time steep decay phase, the shallow decay /plateau phase, normal decay phase and late steep decay phase [?].

2.4.1 Steep decay of early x-ray light curves

. This phase is the tail of prompt emission that governed by curvature effect, for which emission from different viewing angles reaches the observer with different delays due to the light propagation effects [?]. The relationship between temporal and spectral slopes of higher latitude emission is $\alpha = 2 + \beta$. It is independent of any of the environmental or other parameters such as peak frequency and cooling frequency that affects the closure relations for the external shocks.

Swift answer the debate of separation between prompt emission and late afterglow regarding to internal and external origin of the prompt emission i.e internal shocks are the origin of prompt emission [?]. As shown in (Fig2.6 above), slope of early steep decay is around $3 < \alpha_1 < 5$. This phase may be simply the high latitude

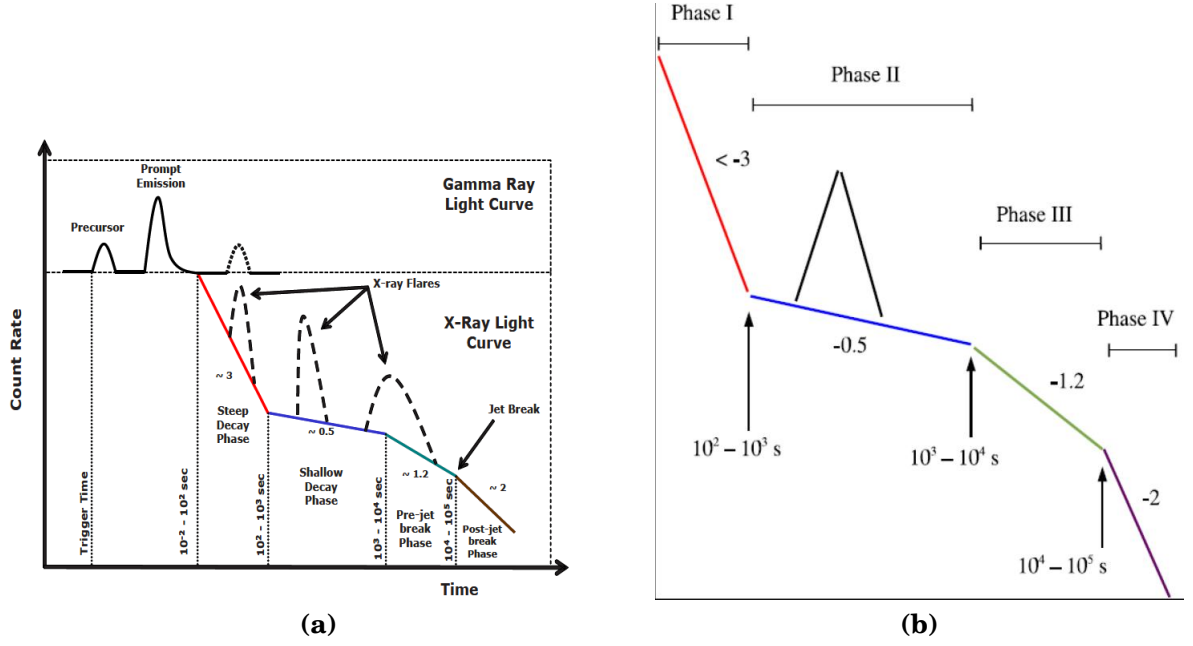


Figure 2.7: (a) Canonical GRB light curve , showing prompt phase followed by afterglow phase.

(b) Canonical x-ray light curves with its components: a steep decay phase (typical index of 3) which can then break to a shallower decline (shallow decay phase), a standard afterglow phase (pre-jet break phase), and possibly, a jet break and post-jet break phase. Sometimes an X-ray flare is seen.

emission associated with the prompt gamma-ray sources at $R \gtrsim 10^{15}$ cm when the central engine turns off faster than the decline of the X-ray light curves . On the other hand, if the emission region is at much smaller radius than the rapidly declining X-ray light curve reflects the time dependence of central engine activity[?].

Detailed analysis of a sample of GRBs suggests that the high latitude "curvature effect" model can explain the early steep decay phase [?]. As we have shown in (Fig 2.6), the achromatic change of phases for sample GRBs indicates the light curves transition. These GRBs followed the decay power law relation $F_\nu \propto t^{-\alpha_1}$ where, $\alpha_1 = 2 + \beta$ for curvature effect model. Generally, this phase has already stayed between the time interval of $10^{-2} - 10^2$ seconds and $10^2 - 10^3$ seconds that presented (in fig 2.6) at the right side.

2.4.2 Shallow /plateau decay X-ray light curves

This phase is sometimes called plateau phase and very small decay with value of decay $0.5 < \alpha_2 < 1.0$. This phase rises when the energy ejected to the decelerated

external shock. When the energy is terminated, the decay of light curves become slow down and the transition to phase three (normal decay) is occurred [51]. In this phase, the shape of light curves in the X-ray and optical bands should be similar where break occur at the same time in these bands.[?] [?] .

There are two acceptable explanations behind the emission mechanisms of this phase. (1) A smooth and gradual energy injection that arrives in the forward shock, is due to the decrease of the Lorentz factor Γ at the end of prompt emission. The mass that is injected to the forward shock is the function of its lorentz factor and the energy injected. As a result Γ increases monotonically with radius,(which we discussed in detail in section (2.6). The flux decays are a power law and depends on the mass and the energy injected . (2) The central engine of the source stays active for hours after the burst and injects the smooth and continues energy at later times, several times after the burst[?] [?] .

X-ray plateaus results from the contribution of prompt X-ray emission scattered by dust in the host galaxy. The optical flux or the powerful outburst episode is already ruled out by the prompt optical data[?] .

2.4.3 normal decay of x-ray light curve

This is the third phase in this canonical phase description. This phase has a decay slope around $1.0 < \alpha_3 < 1.5$ which was expected before swift and it is consistent standard fireball afterglow model in ISM [56]. The explanation of this phase is related to the end of energy injection at the external shocks. This implies (1) the fall of the Lorentz factor of forward shock up to the point of minimal Lorentz factor that carries a significant initial energy. (2) The time that the central engine needs to be in active. In general the normal decay is expected in the standard forward shock.[?]]

2.4.4 Late steep decay following the plateau in X-ray light curves

The early steep decay represented at the left side of fig 2.6 , the decay slope is greater than 2. After the normal decay, X-ray emission is powered by a continues jet from a long lasting central engine. Then X-ray flux from the external shock is buried beneath this emission [58]. Indeed, the canonical X-ray light curve can be matched with the accretion history in the collapsar GRB model. This model assume that the X-ray luminosity is proportional to the accretion power of the central

engine [59]. This late steep decay of swift, represents an achromatic steepening that happens due to the jet breaks. When the Lorentz factor of the ejecta becomes larger than θ_0^{-1} compared to the jet opening angle θ_0 , the ejecta is collimated into a jet break. Finally, this phase is expected in the forward shock model as a jet break. Jet breaks are thought to happen due to the beaming of emission from GRBs. This phase has pre-jet-break phase and post-jet-break phase, (see in Fig 2.6).[?] [?]

2.4.5 Time breaks in swift X-ray afterglow

As shown in (Fig 2.6), there are three break points and the time at that points are called breaking time of afterglow light curves. These break times are the first break time, the second break time and the jet break time.

2.4.6 The first break in the light curve ($t_{break,1}$)

This is the time at which the phase change of light curves from phase I to phase II is took places. As we have shown in (Fig2.6), the $t_{break,1}$ is around $t_{break,1}(10^2 - 10^3)$ s $< t_1 < t_{break,2}(10^3 - 10^4)$ seconds).

The first break time is also the time when the slow decaying emission from the forward shock become dominant over the rapidly decaying flux from the prompt emission at a large angle. In sharply decaying flux, the prompt emission initially dominates over the external shocks at $t > t_{break,1}$ [?].

2.5 Decay of flux with time of observed light curve

The fluence (S) is the total radiant energy collected from the GRBs per unit area over the duration of the event (i.e., T_{90}). It is computed by integrating its energy flux over time and the energy range of the detector (i.e., the total energy collected per unit time and per unit area). The fluence measured between energies E_{min} and E_{max} is given by[Firaol Fana]

$$S = T_{90} \int_{min}^{max} E \frac{dN}{dE} dE \quad (2.1)$$

The energy flux of a burst is defined

$$F = \int_{Emin}^{Emax} E \frac{dN}{dE} dE \quad (2.2)$$

When relativistic, conical and optically thin source moving with a Lorentz factor Γ turns off abruptly, the flux declines rapidly with time [47]. In such type of source which is specified with spherical co-ordinate (r, θ, φ) , the source turned off at $r = R_0$. where r is the radius of the photo/jets, R_0 is the radius of the observer and θ is measured with respect to the line of sight to the observer. The time dependence

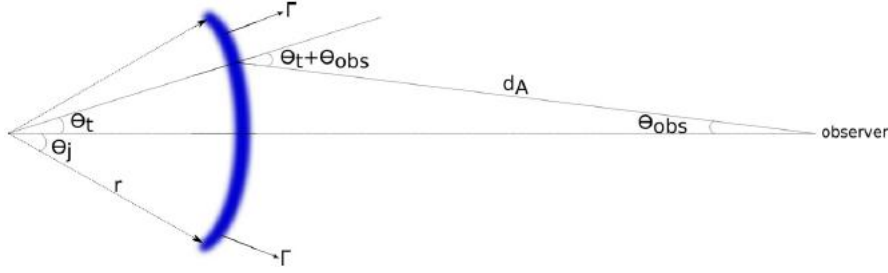


Figure 2.8: A sketch of the various angles and distances for the large angle (or high latitude) emission when the γ -ray source turns off suddenly.

of observed flux follows from the lorentz transformation of specific intensity. The specific flux in the observer frame from the relativistic source of moving object with specific intensity $I_{\nu'}$ and spectrum frequency $\propto \nu'_{-\beta}$ is given by

$$f_{\nu}(t_{obs}) = \int d\Omega_{obs} I_{\nu} \cos\theta_{obs} \quad (2.3)$$

where $d\Omega_{obs}$ is the solid angle of the source, I_{ν} is the specific intensity of the source photon. To derive the standard flux decay of GRBs, let we define $d\Omega_{obs}$ and I_{ν} in the relativistic beaming.

In relativistic beam of photons, the transverse component of the momentum does not change under Lorentz transformation, i.e its comoving and lab frame values are the same. Thus

$$\nu \sin\theta = \nu' \sin\theta' \quad (2.4)$$

or

$$\sin\theta = \frac{\nu'}{\nu} \sin\theta' \quad (2.5)$$

Since the photon frequency on the observer frame, ν , can be expressed in terms of the comoving frequency, ν' , using standard Lorentz transformation of photon as

$$\nu = \frac{\nu'}{\Gamma(1 - \frac{v \cos\theta}{c})} = \nu' D \quad (2.6)$$

where D is standard Doppler effect which is expressed as $[\Gamma(1 - \frac{v \cos \theta}{c})]^{-1}$. Then the ratio of the frequency become $\frac{\nu'}{\nu} = \frac{1}{D}$ and substituting this ratio into Eq. (2.5), we obtain

$$\sin \theta = \frac{\sin \theta'}{D} \quad (2.7)$$

For large Γ , $\theta \approx \frac{\theta'}{\Gamma}$. This tells us photons are focused in the forward direction such that the angular size of photo beam in the lab frame is smaller than it is in the comoving frame by a factor $\sim \Gamma$. And also the solid angle for a canonical beam of photons in lab frame is smaller than in the comoving frame by a factor of $\sim \Gamma^2$. This implies the Lorentz transformation of solid angle is:

$$d\Omega = \sin \theta d\theta d\phi = \frac{\sin \theta' d\theta' d\phi'}{D^2} = \frac{d\Omega'}{D^2} \quad (2.8)$$

The other parameter in the Lorentz transformation is the specific intensity. It is defined as flux per unit frequency and solid angle carried by photos traveling with in a narrow conical beam with its axis perpendicular to surface dA . This means

$$I_\nu = \frac{dE}{d\nu dt_{obs} dA d\Omega} \quad (2.9)$$

Considering $d\nu' dt'_{obs} dA' = d\nu dt_{obs} dA$, are Lorentz invariant and using Eq. (2.8) and $E = \Gamma E'$, Eq. (2.9) can be reduced to

$$I_\nu = D^3 I'_{\nu'} \quad (2.10)$$

Since for intrinsic spectrum, $I'_{\nu'} = I' \nu'^{-\beta}$, where β is spectral index, then the specific intensity is summarized as

$$I_\nu = D^3 \nu'^{-\beta} I' \quad (2.11)$$

This equation, can be simplify by substituting the value of ν' from the Eq. (2.6)

$$I_\nu = D^{3+\beta} \nu^{-\beta} I' \quad (2.12)$$

Finally substituting Eq. (2.8) and Eq. (2.12) into Eq. (2.3) and integrating over $d\phi$ in the interval $0 - 2\pi$, the observed flux becomes

$$f_\nu(t_{obs}) = 2\pi \int d\theta_{obs}$$

Research methodology

Introduction

After the launch of the Swift , observational and theoretical understanding of prompt and afterglow phases of gamma-ray bursts promptly changed due to use of satellites that equipped with improved detecting instruments. Furthermore, the debating issues of GRBs at early discovery: its origin (galactic or cosmological location) , and isotropic distributions of GRBs were confirmed after 2004 in swift era. Not only these , standard models " fire ball " developed during this era to explain the emission mechanisms of gamma-ray burst and its afterglows (from X-ray to radio band). However, as far as review of related litretures (reading of previous papers) concerned , the features of temporal and spectral indices of canonical x-ray afterglow yet unclear. So to fill the knowledge gaps and explain unclear issues mentioned in section 1.5, comprehensive methodology of quantitative and qualitative research and procedures are implemented.

3.1 Research designs

Fireball Models

As we have mentioned in section (2.2), the standard fireball model proposed to explain afterglow gamma-ray bursts. In standard fireball model, the behavior of X-ray light curves assumed to be characterized by a single power law and broken power law decay where flux fading as:

$$f_{\nu}(t) \propto t^{-\alpha} \quad (3.1)$$

where f_{ν} the flux decay with time and α is the temporal index/decay slope and subscripted by numbers $\alpha = 1, 2, 3,$ and 4 for early steep decay slope, shallow decay slope, normal decay slope and late decay slope respectively , that were captured by the swift/XRT. This is the model that relates both temporal (α) and spectral (β)

indices in standard fireball model as:

$$\alpha = 2 + \beta \quad (3.2)$$

is called the closure relation , where both β and α have no units.

spectral models

Several spectral functions are available for use with gtlike. The power-law model is the simplest model that can be used to describe a GRB spectrum . This model consists of two parameters: the low-energy photon index α and the normalization A. With these two parameters, the power-law model can fit the spectra of most GRBs if they are applicable to such a burst. This model is suitable when the signal-to-noise ratio of the fitting spectrum is very low and in the case when the signal is weak and if the break energy cannot be determined due to the break energy of the broken power-law spectrum lying outside the energy band of such a detector (e.g., Cabrera et al. 2007). The power-law spectral model for point source is described by the equation below:[10]

Power law (PL)

$$\frac{dN}{dE} = N_o (dE/E_o)^{-\gamma} \quad (3.3)$$

where the parameters in the XML definition have the following mappings:

Prefactor = N_o

Index = γ

Scale = E_o

and the units are $cm^{-2} s^{-2} MeV^{-2}$. Similarly , the spectral function characterizing diffuse sources defined as:

Broken Power Law (BPL)

And has function of the form:

$$\frac{dN}{dE} = N_o \times \begin{cases} (E/E_b)^{-\gamma_1}, & \text{if } E < E_b. \\ (E/E_b)^{-\gamma_2}, & \text{otherwise.} \end{cases} \quad (3.4)$$

and has units $cm^{-2} s^{-2} MeV^{-2} sr^{-2}$.

where the parameters in the XML definition have the following mappings:

prefactor= N_o

index₁= γ_1

Table 3.1: classes of sampled GRBs with light curve(s): 1,2 and 3 breaks

Class of GRBs	LC with Break 1	LC with Break 2	LC with Break 3	Total
Short GRB	2	3	5	10
Long GRB	3	2	5	10
Total	5	5	10	20

$$index_2 = \gamma_2$$

$$\text{Break value} = E_b$$

3.2 Type of data and its source

For our work , we used the existing secondary data type detected by Swift-XRT (evans et.al Online repository) over longer periods. In our sample , both the classes of gamma-ray bursts (short and long GRBs) are selected equally.

3.3 Data sampling technique and size

Three Criterion were designed to select the required sample. i.e types of gamma-ray bursts , the number of light curve breaks and well defined red shifts are used to select the desired sampled data. Based on mentioned criterion , twenty (20) GRBs afterglows are selected using simple random probability sampling method. Accordingly, the sampled GRBs data afterglows tabulated in table 3.3 below.

3.4 Validity and reliability of data

As mentioned in section 3.3, examine the data then to get the information about object under taken , we already decided to follow both quantitative and qualitative approaches , standared models and tools were proposed to use in analyzing the data collected so as to achieve the desired objectives and give answers for the statements of problems mentioned in section 1.5. This might be keep the validity and reliability of our work.

3.5 Data processing and analyzing

3.5.1 Data processing

As mentioned in section 3.3 above , sample of twenty gamma -ray bursts (long and short) were collected to analyze. To extract relevant information and conclusions that support for final judgment data of the sampled GRBs were cleaned by avoiding duplicated and incorrect data , missing values and outliers.

3.5.2 Data analyzing

Using python 3 program language , graphical relation between X-ray flux (F) and time (t) has been shown for the sampled data. Hereafter considering high latitude radiation and the flux decay closure relations, we made a numerical determinations of temporal and spectral indices of the afterglow decay for early steep decay and temporal index for the rest phases.

A) analysis of short GRBs with 1 or 2 light curve breaks:

I use simple power law

B) analysis of long GRBs with 1 or 2 light curve breaks:

C)analysis of short GRBs with 3 light curve breaks :

D)analysis of long GRBs with 3 light curve breaks:

Result and discussion

4.1 Results

4.2 discussion

Conclusion

Bibliography

Bibliography

DECLARATION

ADDIS ABABA UNIVERSITY
COLLEGE OF NATURAL AND COMPUTATIONAL SCIENCES
DEPARTMENT OF PHYSICS

MSc Thesis

Light Curve Charactersics Of Gamma-Ray Bursts

Name of Candidate: Temam Beyan

I the under signed declare that the thesis is my original work and no part of it can be claimed as an intellectual property of anybody else except me and my advisors.

Signature: _____